HHS Public Access

Author manuscript

Nat Med. Author manuscript; available in PMC 2019 January 09.

Published in final edited form as:

Nat Med. 2018 August ; 24(8): 1268–1276. doi:10.1038/s41591-018-0083-x.

Anatomical and Functional Dichotomy of Ocular Itch and Pain

Cheng-Chiu Huang[1,7,*], **Weishan Yang**[1,*], **Changxiong Guo**[1], **Haowu Jiang**[1], **Fengxian Li**[1,2], **Maolei Xiao**[1], **Steve Davidson**[3], **Guang Yu**[4], **Bo Duan**[5,8], **Tianwen Huang**[5], **Andrew J.W. Huang**[6], and **Qin Liu**[1,6,#]

[1]Department of Anesthesiology and Center for the Study of Itch, Washington University School of Medicine, St. Louis, MO, USA

[2]Department of Anesthesiology, Zhujiang Hospital, Southern Medical University, PR China

[3]Department of Anesthesiology and Pain Research Center, University of Cincinnati College of Medicine, Cincinnati, OH, USA

[4]School of Medicine and Life Sciences, Nanjing University of Chinese Medicine, Jiangsu, China

[5]Dana-Farber Cancer Institute and Department of Neurobiology, Harvard Medical School, Boston, MA, USA

[6]Department of Ophthalmology and Visual Sciences, Washington University School of Medicine, St. Louis, MO, USA

Abstract

Itch and pain are refractory symptoms of many ocular conditions. Ocular itch is generated mainly in the conjunctiva, and is absent from the cornea. In contrast, most ocular pain arises from the cornea. However, the underlying mechanisms remain unknown. Using genetic axonal tracing approaches, we discovered distinct sensory innervation patterns between the conjunctiva and

[#]Correspondence and material requests should be addressed to Q. L. (qinliu@wustl.edu).

[7]Present address: Merck Research Laboratories, South San Francisco, CA, USA

[8]Present address: Department of Molecular, Cellular, and Developmental Biology, University of Michigan, Ann Arbor, MI, USA

[*]These authors contributed equally to this work

Accession Codes:

None

Author Contributions

C.-C.H. performed genetic axonal tracing, pharmacological and behavioral assays, calcium imaging experiments, immunofluorescence staining, data analysis, and participated in manuscript preparation. W.Y. conducted retrograde tracing of ocular afferent neurons and single cell picking, pharmacological and behavioral assays, calcium imaging, immunofluorescence and H&E staining, data analysis, and participated in manuscript preparation. C.G. conducted single cell qRT-PCR, immunofluorescence staining, and participated in mouse breeding strategy design, genetic ablation tests, and manuscript preparation. H. J. did electrophysiological recordings and data analysis.F.L. conducted TRPM8-GFP axonal tracing and ocular pain tests. M.X., in collaboration with W.Y, examined itch-sensing afferent fibers in human conjunctiva. S.D. did the electrophysiological recordings and data analysis. G.Y. conducted calcium imaging of culture DRG neurons. B.D. and T. H. perfused *Slc17a8*$^{cre/+}$; *Rosa26*$^{tdT/+}$ mice and provided tissues for imaging. A. J.W.H. provided human tissues and contributed to experimental design and manuscript preparation. Q.L. planned and directed all of the experiments and wrote the paper.

Competing Interests Statement

The authors declare no competing financial and non-financial interests.

Data Availability Statement

All data generated or analyzed during this study are included in this published article (and its supplementary information files).

cornea. Further genetic and functional analyses in rodent models demonstrate that a subset of conjunctival-selective sensory fibers marked by MrgprA3 expression, rather than corneal sensory fibers, mediates ocular itch. Importantly, the actions of both histamine and non-histamine pruritogens converge onto this unique subset of conjunctiva sensory fibers, and enable them to play a key role in mediating itch associated with allergic conjunctivitis. This is distinct from skin itch in which discrete populations of sensory neurons co-operate to carry itch. Finally, we provide a proof-of-concept that selective silencing of conjunctiva itch-sensing fibers by pruritogen-mediated entry of sodium channel blocker QX-314 is a feasible therapeutic strategy to treat ocular itch in mice. Itch-sensing fibers also innervate the human conjunctiva,and allow pharmacological silence using QX-314.Our results cast new light on the neural mechanisms of ocular itch and open a new avenue for developing therapeutic strategies.

Introduction

Itch is a frequent symptom of many ocular conditions, including allergic conjunctivitis, dry eye and microbial infections[1-3]. Ocular itch, especially that induced by severe ocular allergy such as atopic or vernal keratoconjunctivitis, is often difficult to manage [1,2,4]. Compulsive rubbing or scratching itchy eyes may result in ocular infections or injuries, keratoconus, and even cataracts[5,6].Ocular itch mainly occurs in the conjunctiva, the mucosal membrane lining the inside of the upper and lower eyelids and covering the sclera[2,4]. By contrast, itch is usually absent from the cornea. It is perplexing why itch occurs in the conjunctiva rather than the cornea. Unlike the conjunctiva, the cornea lacks blood vessels and mature immune cells, and is immune-privileged [7,8]. Because the interaction between immune cells and sensory neurons plays an essential role in many types of chronic itch [9,10], the absence of immune cells may underlie the lack of itch in the cornea. However, studies have shown that compounds released from immune cells, such as histamine, are found in the tear fluids which lubricate the cornea as well as the conjunctiva[11,12]; therefore, sensory fibers in the cornea can readily interact with these compounds. The mechanism underlying the conjunctival origin of ocular itch remains unclear.

Similar to but distinct from ocular itch, ocular pain represents another highly prevalent yet challenging clinical problem. Most ocular pain arises from the cornea, as it is uniquely more sensitive to mechanical and other stimuli than other parts of the eye and human body[13,14]. Innocuous mechanical touch or coolness, which does not evoke pain in the conjunctiva or other tissues, is often sufficient for provoking severe pain in the cornea[13-17]. Since the lack of mature immune cells in the cornea unlikely underlies either the conjunctival origin of itch or corneal pain super-sensitivity, we hypothesize that the selective origins of ocular itch and nociception is due to differences in sensory fibers innervation of the cornea and conjunctiva.

Our previous study has revealed an essential involvement of TRPA1-mediated nonhistaminergic itch pathway in allergic ocular itch [18]. However, TRPA1 is expressed by both nociceptive and itch-sensing neurons[19,20]. It is unknown which subsets of TRPA1^{+} sensory neurons are critical for ocular itch, and their innervation patterns in the conjunctiva and cornea. Recent large-scale single-cell RNA sequencing has classified three discrete populations of dorsal root ganglion (DRG) neurons with distinct repertories of itch receptors

[21]. The first population is defined by the expression of itch receptors for β-alanine (MrgprD) and lysophosphatidic acid (LPAR3 and LPAR5), and mediates mechanical pain[22] and skin itch induced by β-alanine and cholestasis associated with elevated lysophosphatidic acid[21,23,24]. The second population is specifically linked to skin itch. These neurons express the itch receptors MrgprA3 and MrgprC11/X1, and detect multiple pruritogens including anti-malaria drug chloroquine, itch-inducing peptides BAM8-22 and SLIGRL, and cathepsin S[21,25-29]. The third population expresses neuropeptide somatostatin (SST) and itch receptors for IL-31, leukotriene D4 (LTD4), and serotonin, and mediates skin itch induced by these pruritogens [21,30]. In addition to itch-sensing neurons, single-cell RNA sequencing also reveals two types of peptidergic nociceptive neurons, and type C low-threshold mechanoreceptors (C-LTMRs) that are involved in mechanical pain and pleasant touch [21,31]. However, it is unclear whether this proposed classification of sensory fibers for DRG neurons also applies to ocular afferents, and whether the selective origins of ocular itch and nociception is attributed to distinct sensory innervation patterns of the cornea and conjunctiva. To address these questions, an in-depth classification of primary sensory neurons, axonal projection and functional characterization of each population in the cornea and conjunctiva are therefore required.

Results

Distinct sensory innervation patterns between the cornea and conjunctiva

Both the conjunctiva and cornea receive the axonal innervation from primary sensory neurons located in the trigeminal ganglia (TG). Based on gene expression profiles, ocular afferent neurons are heterogeneous, and can be grouped into multiple subsets according to the molecular criteria used for classification of DRG neurons [21] (supplemental Table S1). We found that most populations of sensory neurons innervate both the conjunctiva and cornea, as well as the skin, including TRPV1$^+$ heat-sensitive neurons, and neuropeptide CGRP-expressing nociceptive neurons (supplemental Table S2). However, low-threshold mechanosensitive C fiber neurons that express vesicular glutamate transporter 3 (VGLUT3, gene *Slc17a8*)[31,32] selectively innervate the whole-mount cornea but not the conjunctiva (Fig. 1A-C, supplemental Table S2).This selective innervation pattern was further confirmed by section staining and retrograde tracing (supplemental Fig. S1). In addition, we found that cold-sensing TRPM8$^+$ sensory fibers branch extensively and terminate in the superficial layers of the corneal epithelium, but only very few TRPM8$^+$ primary afferent fibers were found in the palpebral conjunctiva (Fig. 1D-F, supplemental Fig. S2, and Table S2).

Finally, among the nine populations examined, two populations of primary sensory neurons were discovered that selectively innervate the conjunctiva but not the cornea (supplemental Table S2 and Fig. 1). The first population specifically expresses MrgprD. Using an *Mrgprd*$^{egfp/+}$ reporter line[33], we found that MrgprD$^+$ sensory fibers innervate the conjunctiva but not the cornea (Fig. 1G-I). Dissimilar to their broad innervation in the skin, MrgprD$^+$ sensory fibers merely innervate the marginal conjunctiva (Fig. 1G-H). This region contacts with the ocular surface during blinking, and is termed the lid wiper[34].

The second population expresses MrgprA3. Using *Mrgpra3*$^{gfp\text{-}Cre}$*; Rosa26*$^{tdTomato/+}$ (*Mrgpra3*^{tdTomato}) mice[26], we found that MrgprA3$^+$ sensory fibers selectively innervate the

conjunctiva, but are completely absent from the cornea and mucosal tissues tested, including nasal and oral mucosa, rectum and vagina (Fig. 1J-O). MrgprA3$^+$ sensory terminals are particularly enriched in the conjunctiva close to the medial and lateral canthi (corners of the eye), regions that are most sensitive to itch. This selective innervation pattern was further confirmed by retrograde tracing (supplemental Fig. S3), suggesting a role of MrgprA3$^+$ sensory fibers in ocular itch. The other population of itch-related sensory neurons that express SST is completely absent from both the conjunctiva and cornea (Fig. 1P-R), despite their dense innervation in the skin (Fig. 1R). Distinct sensory innervation patterns of the cornea and conjunctiva were further confirmed by single cell RT-PCR (Fig. 1S and supplemental Table S1).

A subset of conjunctival-selective sensory fibers mediates ocular itch

To test the hypothesis that ocular itch is mediated by conjunctiva-selective sensory fibers, we studied the function of corneal- or conjunctival-selective sensory neurons in ocular itch. We first examined the involvement of corneal TRPM8$^+$ sensory fibers in ocular itch. Exposing the mouse eyes to cold air flow (13 degree) or menthol (an organic compound from peppermint that selectively activates TRPM8) provokes pain-related blinking and eye-closing responses, rather than itch-related scratching behavior, in wild-type (WT) mice. TRPM8-deficiency entirely abolished pain responses to cold stimuli (supplemental Fig. S4), indicating that TRPM8 mediates corneal cold super-sensitivity.

To further study the function of conjunctival-selective sensory fibers in ocular sensation, we topically applied itch- or pain-inducing chemicals to the lower conjunctival sac in mice[18]. We discovered that IL-31 and LTD4, two immune factors that selectively activate SST$^+$ sensory neurons in the skin[21], failed to generate ocular itch-related scratching or pain-related wiping behavior in mice (Fig. 2A), corroborating the absence of SST$^+$ sensory fibers in the conjunctiva. As a control, IL-31 evokes significant itch in the skin (Fig. 2A), as reported previously[21,30,35]. Next, we examined the role of MrgprD$^+$ neurons in ocular sensation. Using beta-alanine (an MrgprD agonist)as a stimulant, we found that activation of MrgprD$^+$ neurons only evoked minimal ocular scratching (Fig. 2B), arguing against a significant role of these neurons in ocular itch. Since the innervation of MrgprD$^+$ neurons is restricted to the lid wiper region of the conjunctiva (Fig. 1G-H), it supports that these neurons sense eye blinking and tearing, rather than itch.

Finally, we tested the role of MrgprA3$^+$ neurons in ocular itch. We found that ablation of MrgprA3$^+$ sensory neurons (supplemental Fig. S5) significantly reduces ocular itch induced by an array of itch-inducing molecules. Chloroquine, the agonist for MrgprA3 [25], elicits significant ocular itch in WT mice, but not in MrgprA3$^+$ neuron-ablated mice (Fig. 2C). In addition, neuropeptide FF (NPFF), an agonist for itch receptor MrgprC11 [36], also induces ocular itch in an Mrgpr-dependent manner. Ocular itch induced by histamine and serotonin are abolished in MrgprA3$^+$ neuron-ablated mice as well (Fig. 2C). This result is entirely unexpected, as histamine and serotonin can activate MrgprA3-independent itch-sensing fibers in the skin,and ablation of MrgprA3$^+$ neurons cannot completely abolish the skin itch to these pruritogens [21,26,30,37]. Our results demonstrate that ocular itch and skin itch involve

different mechanisms, and MrgprA3$^+$ sensory neurons play a more predominant role in ocular itch than in skin itch.

We further characterized the physiological properties of MrgprA3$^+$ neurons that innervate the conjunctiva by crossing *MrgprA3^{tdTomato}* mice with *Pirt$^{GCaMP3/+}$* mice expressing the calcium indicator GCaMP3 in primary sensory neurons [38].The resulting *Pirt$^{GCaMP3/+}$; Mrgpra3^{tdTomato}* mouse line allows *ex vivo* imaging of calcium mobilization in MrgprA3$^+$ sensory fibers (labeled by tdTomato) in response to pruritogens applied onto the conjunctiva (Fig. 2D-I and S6). Indeed, we discovered that MrgprA3$^+$ fibers respond to a range of itch-inducing chemicals with increased $[Ca^{2+}]_i$, including histamine, serotonin, chloroquine, and NPFF (Fig. 2D-I and S6), correlating well with our *in vivo* behavioral results. Notably, MrgprA3$^+$ sensory neurons innervating the body skin failed to respond to serotonin (supplemental Fig. S7). Instead, MrgprA3-independent SST$^+$ sensory neurons mediate serotonin-induced itch in the skin [30]. Our results thus support that MrgprA3$^+$ sensory fibers in the conjunctiva incorporate a partial function of SST$^+$ sensory neurons and are different from those innervating the skin (Fig. 2J), providing a molecular basis for the predominant role of MrgprA3$^+$ sensory neurons in ocular itch.Interestingly, histamine, serotonin and NPFF have been reported to be secreted from mast cells [36,39,40], suggesting that conjunctival MrgprA3$^+$ sensory neurons might detect itch mediators from mast cells in allergy, and mediate ocular itch associated with allergic conjunctivitis (Fig. 2J). Indeed, conjunctival allergen challenge elicited significant mast cells degranulation and scratching behavior directed to the treated eye in immunized WT mice (Fig. 3A-C). Importantly, we found that mast cells are closely associated with MrgprA3$^+$ sensory fibers in the conjunctiva (Fig. 3D-E). Upon degranulation of mast cell, granules directly interact with MrgprA3$^+$ sensory fibers (Fig. 3F). Ablation of MrgprA3$^+$ neurons significantly reduced allergic ocular itch (Fig. 3G), indicating that MrgprA3$^+$ sensory fibers are the principal itch-sensing fibers for inflammatory mediators released by conjunctival mast cell in this allergic conjunctivitis model.

The central neural circuit for ocular itch

Studies have revealed distinct central representations for sensory fibers innervating either the conjunctiva or cornea [41]. However, it is unclear whether this anatomical difference underlies the conjunctival origin of ocular itch and corneal insensitivity to itch. Neuromedin B (NMB) is a bombesin-related peptide, and is highly expressed in small-diameter sensory neurons including MrgprA3$^+$ neurons [42,43]. Its function in pain and itch,however, remains controversial[42,44]. Interestingly, we found that NMB is highly expressed in the sensory neurons innervating the conjunctiva but not the cornea (Fig. 4A-G). Importantly, *Nmb*-null mice display significantly reduced ocular itch (Fig. 4I), but normal ocular pain responses, suggesting that NMB is required for itch signal transmission from ocular afferent fibers. Furthermore, NMBR, the receptor for NMB,is found in the central projection area of sensory fibers innervating the conjunctiva as well as the neighboring area that may receive sensory inputs from the skin sensory fibers (such as those from the eyelid skin) (Fig. 4J). However, NMBR is completely absent from the central projection area of the cornea (Fig. 4H). Similar to NMB deficiency, deletion of NMBR leads to a significant reduction in ocular itch (Fig. 4I). These results indicate that NMB/NMBR signaling is required for conjunctival

itch transmission, providing a novel central mechanism for why the cornea is not “itch”-sensitive.

Development of a novel therapeutic strategy for allergic ocular itch

To test whether selective silencing of MrgprA3$^+$ sensory fibers using pharmacological approaches is a feasible therapeutic strategy to provide sustained relief of ocular itch,we adopted an approach of reversibly silencing MrgprA3$^+$ fibers by targeted delivery of a charged sodium-channel blocker, QX-314. QX-314 is membrane-impermeable, and can only enter the cell through large pores of ion channels opened upon neuronal excitation[45,46]. Because TRPA1 is the downstream transduction channel of MrgprA3 [47], QX-314 would be able to permeate into MrgprA3$^+$ neurons via the opening of TRPA1 upon chloroquine challenge (Supplemental Fig. S8A). Indeed, using *Mrgpra3^{tdTomato}* mice, we confirmed that chloroquine-mediated activation of TRPA1 channels allows sufficient QX-314 uptake to suppress voltage-dependent inward sodium currents in MrgprA3$^+$ neurons (Supplemental Fig. S8B-E). This reduction in sodium currents was sufficient to suppress the generation of action potentials in MrgprA3$^+$ neurons (Fig. 5A-D). Furthermore, application of a low concentration of chloroquine (4 mM, supplemental Fig.S9) and QX-314 (1%, 2 μl) onto the conjunctiva effectively suppressed subsequent ocular itch induced by chloroquine (12 mM) applied 30 min later (Fig. 5E), suggesting that conjunctival MrgprA3$^+$ sensory fibers can be silenced *in vivo*. Importantly, this pretreatment of QX-314 with chloroquine remarkably alleviated allergic ocular itch in mice for more than 24 hours, and its efficacy diminished through the next 24 hours (Fig. 5F). In contrast, the anti-itch effects of an antihistamine, pheniramine,diminished within one hour (Fig. 5G). Thus, selective silencing of MrgprA3$^+$ sensory fibers provides more potent and sustained relief of allergic ocular itch than the conventional antihistamine (Fig. 5H).

We next examined the effects of silencing itch-sensing fibers on migration/infiltration and activation of immune cells (particularly mast cells). Allergen challenge induces extensive mast cell accumulation and degranulation (Fig. 5I-K). Silencing of MrgprA3$^+$ sensory fibers effectively diminished mast cells accumulation (Fig. 5I-J), but did not reduce mast cell degranulation. In contrast, pheniramine did not affect mast cell accumulation or immune cell infiltration (Fig. 5I-K). To investigate the mechanisms underlying the immune regulatory effect of silencing itch-sensing afferent fibers, we tested whether MrgprA3$^+$ sensory neurons produce neuropeptides capable of attracting immune cells. Although substance P can directly activate mast cells[48,49], it was not expressed in MrgprA3$^+$ neurons (supplemental Fig. S10), consistent with our single cell qRT-PCR results (supplemental Table 1) and previous findings[26]. In contrast, we detected the expression of neuropeptide CGRP in MrgprA3$^+$ neurons (Fig. 5L). The administration of CGRP peptide into the mouse conjunctiva sac unexpectedly recruited more mast cells, but did not cause mast cell degranulation or itch (Fig. 6M-N).

Conserved innervation pattern and function of itch-sensing afferent fibers in human conjunctiva

Our finding of mouse MrgprA3$^+$ sensory fibers in ocular itch raises the question of whether human Mrgpr-expressing sensory fibers play a similar role in itch perception. Among all the

human Mrgprs, hMrgprX1 is sensitive to chloroquine and corresponds to mouse MrgprA3[25]. Hence, we examined the innervation pattern of hMrgprX1$^+$ sensory fibers in the eye utilizing a newly-generated anti-hMrgprX1 antibody. The antibody selectively stained sensory neurons of *MRGPRX1;Mrgpr-clusterΔ*$^{-/-}$ mice in which hMrgprX1, instead of mouse Mrgprs, is expressed in mouse sensory neurons, but not those from *Mrgpr-cluster Δ*$^{-/-}$ mice (Fig. 6A-B), indicating that the antibody specifically recognizes hMrgprX1. Using this antibody, we found that hMrgprX1$^+$ sensory fibers selectively innervate the conjunctiva, but not the cornea of human eyes (Fig. 6C-D), correlating well with the innervation pattern of itch-sensing fibers in mice.

To determine whether the activation of hMrgprX1 allows the entry of QX-314 via TRPA1 channels, we examined whether TRPA1 is the downstream transduction channel of hMrgprX1 in TG sensory neurons from *MRGPRX1;Mrgpr-clusterΔ*$^{-/-}$ mice. We found that the chloroquine triggered a train of action potentials in hMrgprX1-expressing sensory neurons (identified by calcium imaging, Fig. 6E-F). Importantly, pretreatment of TRPA1 antagonist HC030031 effectively suppressed the neuronal discharge in response to chloroquine (Fig. 6E-F), indicating that TRPA1 is the downstream transduction channel of hMrgprX1 and required for the depolarization of hMrgprX1$^+$ neurons. We further examined the feasibility of selectively silencing hMrgprX1$^+$ sensory fibers using QX-314 for itch treatment. We found that neuronal silencing is effective in alleviating allergic ocular itch in *MRGPRX1;Mrgpr-clusterΔ*$^{-/-}$ mice (Fig.6G). The anti-itch effect lasts for at least 24 hours in this humanized mouse model (Fig.6G).Importantly, QX-314 mediated neuronal silencing is ineffective in *Mrgpr-clusterΔ*$^{-/-}$ mice (Fig. 6G), due to a lack of Mrgprs required for chloroquine-mediated entry of QX-314 into ocular itch fibers, demonstrating the specificity of this neuronal silencing approach. Notably, deficiency in Mrgprs significantly reduces ocular itch in *Mrgpr-clusterΔ*$^{-/-}$ mice, suggesting an indispensable role of Mrgprs in mediating ocular itch. This itch defect can be entirely rescued by the expression of hMrgprX1 in *MRGPRX1;Mrgpr-clusterΔ*$^{-/-}$ mice (Fig.6G), indicating that hMrgprX1 mediates ocular itch and provides a new drug target for ocular itch.

To understand the mechanism by which hMrgprX1 mediates allergic ocular itch, we examined whether hMrgprX1 can be activated by itch mediators released from mast cells in allergy. Our previous study has shown that neuropeptide FF (NPFF) can be released from mast cells and activate sensory neurons via mouse MrgprC11[36]. Here, we found that NPFF also activates hMrgprX1 as revealed by calcium imaging (Fig.6H). Importantly, NPFF induces significant ocular itch in a mouse Mrgpr/ hMrgprX1-dependent manner (Fig. 6I). These data suggest that hMrgprX1 is capable of detecting the itch mediators (such as NPFF) released from mast cells, providing one of the mechanisms by which hMrgprX1 mediates allergic ocular itch. Together, our results indicate that hMrgprX1 is a principal itch receptor for ocular itch and hence a promising drug target for itch management.

Discussion

The findings of conjunctiva- and cornea-selective sensory innervations significantly advance our understanding of the neural basis underlying the dichotomy of ocular itch and pain. The conjunctiva plays an important role in immune surveillance and helps prevent the entrance of

microbes into the eye. The selective projection of itch-sensing fibers to the conjunctiva enables the peripheral sensory system to monitor immune homeostasis and initiate an alarm when the immune system is dysregulated. Indeed, itch is closely associated with many types of immune disorders in the conjunctiva, including allergy, infection and inflammation. By contrast, to maintain its transparency for refracting light and focusing our vision, the cornea lacks blood vessels and is immune privileged [7,8]. Hence, the immune surveillance function of itch-sensing fibers is not required for the cornea. Moreover, the cornea is very fragile and easily damaged. Studies have shown that chronic eye rubbing causes corneal thinning and keratoconus, a condition in which the shape of the cornea becomes irregular or conical.As a protective mechanism, the cornea is densely innervated by subsets of primary sensory fibers, and generates pain in response to normally innocuous stimuli. Our finding of the lack of itch-sensing fibers and NMB/NMBR-dependent itch pathway in the cornea offers an extra protective mechanism to prevent the cornea from being itchy. This newly described mechanism combined with the corneal super-sensitivity effectively protects our cornea from mechanical damages caused by scratching or rubbing.

The finding of conjunctiva-selective itch sensory fibers provides promising and unique neural targets for the development of new anti-ocular itch therapeutic strategies. We provide a “proof-of-concept” that silencing conjunctival itch-sensing fibers effectively alleviates ocular itch. This novel therapeutic strategy is conceptually specific and promises to be safe for the following reasons.

First, pharmacological silencing conjunctival itch-sensing fibers exhibits a more sustained anti-itch effect than antihistamines currently used to treat ocular itch. Different from the binding of antihistamines to histamine receptors at the cell surface, the entry of QX-314 into conjunctival sensory fibers avoids washing off by tear fluid and leads to sustained itch relief. Furthermore, silencing itch-sensing fibers reduces mast cell migration and accumulation at the allergen-challenging site, and hence would decrease the amount of itch mediators released by mast cells, resulting in less severe itch. This neuro-immune interaction offers a novel explanation for the vicious cycle of itching and inflammation. Second, selective silencing of a highly-restricted population of itch-sensing afferent fibers in the conjunctiva circumvents common side-effects caused by antihistamines or immunosuppressive corticosteroids and cyclosporine, including dry eye, glaucoma, cataract and ocular infections. Finally, this strategy would not affect the function of other conjunctival sensory fibers or corneal sensory fibers, which regulate basal tearing and protect the integrity of ocular surface from potential injuries [50,51].

To develop new therapeutic strategies for allergic itch in humans, it is important to translate our discoveries from mice to humans. Despite the large size of the Mrgpr family in mice, there are only seven Mrgprs in humans. Interestingly, hMrgprX1 is sensitive to chloroquine and peptide BAM8-22, both of which elicit histamine-independent itch in humans[25,28,52]. Our finding of selective projection of hMrgprX1-expressing sensory fibers to the conjunctiva but not the cornea in humans substantiates the pathogenic role of this population of neurons in ocular itch. Utilizing *MRGPRX1;Mrgpr-clusterΔ*$^{-/-}$ mice, we confirmed the feasibility of pharmacological silencing of hMrgprX1^{+} sensory fibers using QX-314 for treating allergic ocular itch. Furthermore, we found that hMrgprX1 functions as a principal itch receptor in

ocular allergy, suggesting that hMrgprX1 itself is a promising anti-itch drug target in addition to being a useful molecular marker for itch afferent fibers in the conjunctiva. It would be important to develop potent and specific antagonists of hMrgprX1 for itch management in the future. The humanized mouse model *MRGPRX1;Mrgpr-clusterΔ*$^{-/-}$ will facilitate pharmacological study of the anti-itch effects of hMrgprX1 antagonists *in vivo*, and help yield key pre-clinical evidence.

Online Methods

Animals

C57BL/6J wild-type (Stock#: 000664), B6;129S6-*Gt(Rosa)26Sor*$^{tm14(CAG-tdTomato)Hze}$/J (*Rosa26*^{tdTomato}; Stock#:007908), C57BL/6-*Gt(Rosa)26Sor*$^{tm1(HBEGF)Awai}$/J (*Rosa26*^{HBEGF}; Stock#:007900), B6N.Cg-*Sst*$^{tm2.1(cre)Zjh}$/J (Stock#: 018973) and B6N(Cg)-*Nmb*$^{tm1.1(KOMP)Vlcg/J}$ mice (Stock#:025862) were ordered form the Jackson Laboratory (Bar Harbor, ME). *Mrgpra3*$^{gfp\text{-}Cre}$, *Pirt*$^{GCaMP3/+}$ and *MRGPRX1;Mrgpr-clusterΔ*$^{-/-}$ mice were generous gifts from Dr. Xinzhong Dong of Johns Hopkins University. *Mrgprd*$^{egfp/+}$ mice were from Dr. David J. Anderson of the California Institute of Technology. *Trpm8*$^{gfp/+}$ mice were from Dr. Gina Story. *Nav1.8*^{Cre}, *Nmb*$^{-/-}$, *Nmbr*$^{-/-}$, and *Nmbr*^{gfp} transgenic mice were from Dr. Zhou-Feng Chen of Washington University in St. Louis. *Slc17a8*$^{Cre/+}$ tissues were from Dr. Qiufu Ma of Dana-Farber Cancer Institute. Animals used for behavioral tests were backcrossed to the C57BL/6J background for at least 10 generations and maintained in the congenic background. Male mice (two to three months old) were used for behavioral tests. All animal experiments were performed under protocols approved by Institutional Animal Care and Use of Washington University School of Medicine.

Reagents

Chloroqine (C6628), histamine (H7250), β-Alaine (A9920), serotonin (H9523), QX-314 (L5783), ovalbumin (A5503), DMEM/F12 (D6421), normal goat serum (G9023) and paraformaldehyde (P6148) were all purchased from Sigma-Aldrich (St. Louis, MO). Type I collagenase (17100017), dispase (17105051), anti-GFP antibody (A11122, Lot#1925070; used at 1:1000 dilution), and Alexa Fluor® 488-conjugated goat anti-rabbit antibody (A11008, Lot#1797971; used at 1:1000 dilution), FITC-conjugated avidin (434411, Lot#1561410A; used at 1:1000 dilution), Rhodamine-conjugated avidin (A003-00, Lot#2496; used at 1:400 dilution), DiI (C7000), Alexa Fluor™ 488 Conjugated WGA (W11261), Alexa Fluor™ 555 Conjugated WGA-555 (W32464) and Imject Alum Adjuvant (PI77161) were purchased from Thermo Scientific (Asheville, NC). Leukotriene D_4 (20310) was purchased from Cayman Chemical (Ann Arbor, MI). IL-31 (200-31) was purchased from PeproTech (Rocky Hill, NJ). Chicken anti-GFP (GFP-1020, Lot#GFP697986; used at 1:1000 dilution) was purchased from Aves Lab (Tigard, Oregon).anti-DTR antibody (AF259NA, Lot#PX0911111; used at 1:200 dilution) was purchased from R&D Systems (Minneapolis, MN)[53]. anti-CGRP antibody (6009N T-4239, Lot#040269-6; used at 1:1000 dilution) was purchased from Peninsula Laboratories International, Inc. (San Carlos, CA)[53-55]. X-Gal staining kit (A10300K) was purchased from Genlantis (San Diego, CA). Anti-hMrgprX1 antibody (used at 1:1000 dilution)was generated by Liang Han in Dr. Xinzhong Dong at the Johns Hopkins School of Medicine in Baltimore, MO. Cy5-

conjugated donkey anti-goat antibody (705175147, Lot#131485; used at 1:500 dilution) was purchased from Jackson ImmunoResearch Laboratories, Inc. (West Grove, PA). OCT embedding compound (4583) was purchased from Sakura Finetek USA, Inc. (Torrance, CA). Diphtheria Toxin (150) was purchased from List Biological Laboratories, Inc. (Campbell, CA).

Histology

Discarded cadaveric human donor corneal rims containing peripheral cornea, limbus and peri-limbal conjunctiva from healthy donors were obtained from Dr. Andrew JW Huang after corneal transplantation. The use of human tissue in research conformed to the provisions of the Declaration of Helsinki and was exempted by the Washington University Human Subjects Protection Office. Medical and ocular histories of the donor had been de-identified and reviewed to ensure no evident ocular or systemic diseases. The procurement of donor corneas was performed under a standard protocol by the eye bank of Mid-America Transplants (St. Louis, MO).

All mice used for histology were anesthetized with ketamine/xylazine cocktail and transcardially perfused with ice cold PBS followed by ice cold 4% PFA. Whole mount corneal, oral mucosal, rectal, vaginal, conjunctiva, skin, and DRG tissues were dissected and imaged immediately using Nikon Ti-E microscope. Tissues used for frozen section were post-fixed in ice-cold PFA (4%, 0.5 hr for the conjunctiva; 2%, 2 hr for the skin; 3 hr for the brain and 4%, 20 min for DRGs) and cryoprotected in 30% (w/v) sucrose/PBS solution for 24 hours before they were embedded and frozen in OCT compound.

Tissues were sectioned at 20 μm using a Leica CM-1950 cryostat, allowed to air dry 1 hour, and washed using PBS containing 0.1% Triton-X 100 (PBST). Tissue sections carrying endogenous fluorescence were directly mounted using Fluoromount-G. Tissue sections that required staining were blocked using 10% normal goat serum for 1 hour at room temperature and incubated in primary antibody at 4˚C overnight followed by secondary antibody at room temperature for 2 hours. X-Gal staining was performed according to manufacturer's guide. For mast cell staining, tissue sections were incubated with FITC or rhodamine-conjugated avidin for 15 minutes at room temperature. After staining, tissue sections were mounted using Fluoromount-G and imaged after drying.

Retrograde labeling

WGA (1-2 μL) was injected into the stroma of the cornea or the submucosa of the palpebral conjunctiva of anesthetized mice using pulled glass micropipettes. Animals were euthanized for tissue collection 48-60 hours after the injections.

DiI retrograde neuronal labeling was performed as previously described[56]. In short, ~0.5 μL of 30 ng/μL DiI were injected into the palpebral conjunctival of both lower eyelids of anesthetized mice using a glass micropipette. Animals were used for histology five days after DiI injection.

Cell picking

WGA labeled trigeminal neurons were harvested from adult mice (6–8 week old, both males and females) and pooled into DMEM/F12 media supplemented with 10% fetal bovine serum and antibiotics (DH10). Afterwards, DRGs were digested using a collagenase/dispase solution at 32°C for 20 minutes, triturated, pelleted, and resuspended in 400 μl of DH10 media, per mouse. 200 μl of the cell suspension were then carefully pipetted on top of 1.2 mL of freshly prepared 15% bovine serum albumin (BSA) in a 1.5 mL microcentrifuge tube, and centrifuged at 400 g for 4 minutes to separate neurons from myelin and debris. After purification, the BSA supernatant was aspirated and the pelleted neurons were resuspended in DH10 media. All steps after digestion were performed on ice.

Cells were isolated manually using a controlled cell-picking setup, constructed in-house around a Leica DMi6000 inverted epifluorescent microscope (Buffalo Grove, IL) and a Narishige MMO-202ND micromanipulator (Amityville, NY). WGA labeled neurons were captured into pulled glass micropipettes with 20 micron wide openings and ejected into PCR tubes containing 10 μl of lysis buffer and RNase inhibitor.

Real-Time Quantitative Reverse Transcription PCR

cDNA library from single neurons were generated using Invitrogen SuperScript III CellsDirect cDNA Synthesiss Kit (ThermoFisher 18080300) and as previously described[57]. In short, manually isolated neurons were collected into 0.2 mL thin-walled PCR tubes prefilled with 10 μl supplied lysis buffer and RNase inhibitor; and were flash frozen on dry ice and stored at -80°C until cDNA synthesis. DNase digestion was performed for all cells. First-strand cDNA was generated using 100 nmols (50 mM, 2μl) of oligo$(dT)_{20}$. All other steps were performed according to the manufacturer's protocol.

qPCR was performed using power SYBR Green master mix (ABI 4368702) on an ABI StepOnePlus qPCR machine. Single cell genomic DNA was used as the negative controls and FACS isolated DRG neurons (~36,000 neurons, diluted 1:36,000) was used as the positive control. *Gapdh* was used to identify and exclude samples without input or with failed cDNA synthesis. All primer sets were validated before use, and PCR products were selected for further sequence validation. All gene expression data is presented as folds of *Gapdh* expression, calculated using 2ˆ-(Ct(target Gene)-Ct(Gapdh)).

Behavioral Assays

All animal behavioral experiments were performed and analyzed in blinded manner. Ocular itch experiments were performed as described previously[56]. In short, two to three months old mice were manually restrained and 2.5 μL of pruritogens were applied directly into the inferior conjunctival sac. Afterwards, animals were returned to recording chambers and filmed for 30 minutes. Scratch bouts directed at the treated conjunctiva were scored after completion of filming.

In the ocular cold pain tolerance assays, acclimated test animals were manually restrained and a 0.5L/min stream of temperature controlled air was applied directly to the exposed corneas. Blinking, eye closure and other responses were quantified afterwards.

Mast cell-dependent allergy model were generated as described previously[56]. In short, mice were given two intraperitoneal (*i.p.*) injections of 1:1 mixture of 0.01%(w/v) ovalbumin (OVA) /Imject Alum ten days apart to induce allergic sensitivity to OVA. Seven days after the second *i.p.* injection, sensitized animals were used for behavioral experiments and challenged with 250 μg of OVA to induce allergic ocular itch. To pharmacologically silence itch-sensing fibers in the conjunctiva, 2 μl mixture solution (1% QX-314 + 4 mM chloroquine) was applied to the lower conjunctival sac of immunized mice, before OVA challenging. As a positive control, 0.4% pheniramine was used as a pretreatment to suppress histamine-dependent itch signaling in the conjunctiva. 10 min, 30 min, 1h, 24h or 48h after pretreatments, mice were challenged with OVA, video-recorded for 30 minutes, and quantified blindly.

Mice used in the MrgprA3^{+} neuron ablation model were generated using a protocol adapted from previously published literature[56]. Two months old *Mrgpra3*$^{gfp\text{-}cre+}$*; Rosa26*$^{HBEGF/+}$ mice and *Rosa26*$^{HBEGF/+}$ control littermates were given two *i.p.* injections of 30 μg/kg diphtheria toxin (DTX) three days apart (HBEGF is the gene for diphtheria toxin receptor, DTR). Treated animals were used for behavioral experiments four weeks after the second DTX injection.

Calcium Imaging

Whole mount calcium imaging of the conjunctiva was performed as described previously[56]. In short, conjunctivae were dissected and allowed to recover in oxygenated recording buffer at room temperature for 30 minutes. After recovery, dissected explants were imaged using a Nikon Ti-E inverted microscope and Photometrics CoolSnap HQ_2 CCD camera (Tucson, AZ). The responses of conjunctival sensory fibers to pruritogens were defined as changes in GCaMP3 fluorescence intensity ($\Delta F/F_0$) using the Nikon NIS Elements AR software.

Calcium imaging of cultured dorsal root ganglia (DRG) neurons were performed as described previously[57]. DRGs were harvested from euthanized three to four weeks old mice and pooled in DMEM/F12 media supplemented with 10% fetal bovine serum and antibiotics (DH10). Afterwards, DRG_S were digested using a collagenase/dispase solution at 37˚C for 30 minutes, triturated, pelleted, and resuspended in DH10 media. Afterwards, dissociated DRGs were seeded onto poly-D-lysine and laminin coated glass coverslips, supplemented with 20 ng/ml nerve growth factor and 50 ng/ml glial cell derived growth factor, and cultured at 37˚C for 18-24 hours before use.

Electrophysiology

Cultured sensory neurons expressing tdTomato fluorescence were viewed under an epifluorescent BX50 Olympus microscope. Cells were bathed at room temperature (22 ± 2°C) in external solution containing (in mM): 145 NaCl, 3 KCl, 2.5 $CaCl_2$, 1.2 $MgCl_2$, 7 glucose, and 10 HEPES, adjusted to pH 7.4 with NaOH and 305 mOsm with sucrose. Borosilicate, filamented glass electrodes with 1.7-3.5 MΩ resistance contained (in mM): 130 K-gluconate, 5 KCl, 5 NaCl, 3 Mg-ATP, 0.3 EGTA, 10 HEPES, adjusted to pH 7.3 with KOH and 295 mOsm with sucrose. Pipette potential was zeroed before seal formation, cell capacitance was cancelled electronically, and series resistance was compensated ≥70%.

After gigaseal formation and break-in, chloroquine (200 μM) was bath applied with 5 mM QX-314 in voltage-clamp mode followed by a series of voltage steps while evoked current was monitored. For sodium currents, neurons were held at -70mV and 100ms voltage steps were delivered increasing by 5mV until +35mV was reached. Data were collected with a HEKA EPC 10 amplifier (Heka Electronic, Lambrecht/Pfalz, Germany), digitized at 20 kHz, and recorded on a PC running Patchmaster software (v2; Heka Electronic).

Whole-cell current-clamp recordings of TG neurons from *MRGPRX1;Mrgpr-clusterΔ*$^{-/-}$ mice were performed using a MultiClamp 700B amplifier and pCLAMP 10.5 software (Axon Instruments, U.S.).

Statistical Analysis

All histology, calcium imaging, and electrophysiology experiments were repeated using tissues from at least 3 different mice. All attempts at replication were successful.Sample sizes for itch and pain behavior tests were selected based on power analysis of related publications[56-58] and "sample size determination"[59] (more details in Life Sciences Reporting Summary). Animals were placed into experimental groups based either on their genotype (no randomization) or through simple randomization. Itch and pain behaviors were scored by researchers blinded to mouse genotypes or treatment condition. No animal or data point was excluded from analysis. All data are presented as mean ± s.e.m. F test was used to evaluate whether the variance similar between the groups that are being statistically compared. Statistical significances were determined using two-tailed Student's *t* test (for two groups)or one-way analysis of variance (ANOVA, for three or more groups). Differences were considered significant if *P* value was 0.05 or less.

Life Sciences Reporting Summary

Further information on statistical parameters, software and code, data, study design, materials & experimental systems is available in the Life Sciences Reporting Summary.

Supplementary Material

Refer to Web version on PubMed Central for supplementary material.

Acknowledgments

We are grateful to M.W.Panneton, H. Hu, B. Kim, Z.F. Chen, T. P. Margolis, and X. Dong for insightful discussions and comments on the manuscript,A.S. Yoo and Y. Liu for technique support.

This work was supported by "Research to Prevent Blindness" (RPB) unrestricted grant to the department of Ophthalmology (A.J.W.H., and Q.L.), the National Institutes of Health (R01EY024704 and 1R01AI125743) and Pew Scholar Award to Q.L.

References

1. Ciprandi G, Buscaglia S, Cerqueti PM, Canonica GW. Drug treatment of allergic conjunctivitis. A review of the evidence. Drugs. 1992; 43:154–176. [PubMed: 1372215]
2. Abelson MB, Smith L, Chapin M. Ocular allergic disease: mechanisms, disease sub-types, treatment. Ocul Surf. 2003; 1:127–149. [PubMed: 17075644]

3. Wong AH, Barg SS, Leung AK. Seasonal and perennial allergic conjunctivitis. Recent Pat Inflamm Allergy Drug Discov. 2009; 3:118–127. [PubMed: 19519588]
4. Ono SJ, Abelson MB. Allergic conjunctivitis: update on pathophysiology and prospects for future treatment. J Allergy Clin Immunol. 2005; 115:118–122. [PubMed: 15637556]
5. Yeniad B, Alparslan N, Akarcay K. Eye rubbing as an apparent cause of recurrent keratoconus. Cornea. 2009; 28:477–479. [PubMed: 19411974]
6. Nagaki Y, Hayasaka S, Kadoi C. Cataract progression in patients with atopic dermatitis. J Cataract Refract Surg. 1999; 25:96–99. [PubMed: 9888084]
7. Ambati BK, et al. Corneal avascularity is due to soluble VEGF receptor-1. Nature. 2006; 443:993–997. [PubMed: 17051153]
8. Cursiefen C. Immune privilege and angiogenic privilege of the cornea. Chem Immunol Allergy. 2007; 92:50–57. [PubMed: 17264482]
9. Paus R, Schmelz M, Biro T, Steinhoff M. Frontiers in pruritus research: scratching the brain for more effective itch therapy. J Clin Invest. 2006; 116:1174–1186. [PubMed: 16670758]
10. Oetjen LK, et al. Sensory Neurons Co-opt Classical Immune Signaling Pathways to Mediate Chronic Itch. Cell. 2017; 171:217–228. e213. [PubMed: 28890086]
11. Bonini S, et al. Conjunctival provocation test as a model for the study of allergy and inflammation in humans. Int Arch Allergy Appl Immunol. 1989; 88:144–148. [PubMed: 2651314]
12. Leonardi A. The central role of conjunctival mast cells in the pathogenesis of ocular allergy. Curr Allergy Asthma Rep. 2002; 2:325–331. [PubMed: 12044269]
13. Belmonte C, Acosta MC, Schmelz M, Gallar J. Measurement of corneal sensitivity to mechanical and chemical stimulation with a CO2 esthesiometer. Invest Ophthalmol Vis Sci. 1999; 40:513–519. [PubMed: 9950612]
14. Muller LJ, Marfurt CF, Kruse F, Tervo TM. Corneal nerves: structure, contents and function. Exp Eye Res. 2003; 76:521–542. [PubMed: 12697417]
15. Tanelian DL, Beuerman RW. Responses of rabbit corneal nociceptors to mechanical and thermal stimulation. Exp Neurol. 1984; 84:165–178. [PubMed: 6705882]
16. MacIver MB, Tanelian DL. Structural and functional specialization of A delta and C fiber free nerve endings innervating rabbit corneal epithelium. J Neurosci. 1993; 13:4511–4524. [PubMed: 8410200]
17. Beuerman RW, Tanelian DL. Corneal pain evoked by thermal stimulation. Pain. 1979; 7:1–14. [PubMed: 503550]
18. Huang CC, et al. A histamine-independent itch pathway is required for allergic ocular itch. J Allergy Clin Immunol. 2016; 137:1267–1270. e1261–1266. [PubMed: 26521042]
19. Bautista DM, et al. TRPA1 mediates the inflammatory actions of environmental irritants and proalgesic agents. Cell. 2006; 124:1269–1282. [PubMed: 16564016]
20. Wilson SR, et al. TRPA1 is required for histamine-independent, Mas-related G protein-coupled receptor-mediated itch. Nat Neurosci. 2011; 14:595–602. [PubMed: 21460831]
21. Usoskin D, et al. Unbiased classification of sensory neuron types by large-scale single-cell RNA sequencing. Nat Neurosci. 2015; 18:145–153. [PubMed: 25420068]
22. Cavanaugh DJ, et al. Distinct subsets of unmyelinated primary sensory fibers mediate behavioral responses to noxious thermal and mechanical stimuli. Proc Natl Acad Sci U S A. 2009; 106:9075–9080. [PubMed: 19451647]
23. Kremer AE, et al. Lysophosphatidic acid is a potential mediator of cholestatic pruritus. Gastroenterology. 2010; 139:1008–1018. 1018–e1001. [PubMed: 20546739]
24. Liu Q, et al. Mechanisms of Itch Evoked by beta-Alanine. The Journal of neuroscience : the official journal of the Society for Neuroscience. 2012; 32:14532–14537. [PubMed: 23077038]
25. Liu Q, et al. Sensory Neuron-Specific GPCR Mrgprs Are Itch Receptors Mediating Chloroquine-Induced Pruritus. Cell. 2009:1353–1365. [PubMed: 20004959]
26. Han L, et al. A subpopulation of nociceptors specifically linked to itch. Nat Neurosci. 2013; 16:174–182. [PubMed: 23263443]
27. Liu Q, et al. The distinct roles of two GPCRs, MrgprC11 and PAR2, in itch and hyperalgesia. Sci Signal. 2011; 4:ra45. [PubMed: 21775281]

28. Sikand P, Dong X, LaMotte RH. BAM8-22 peptide produces itch and nociceptive sensations in humans independent of histamine release. The Journal of neuroscience : the official journal of the Society for Neuroscience. 2011; 31:7563–7567. [PubMed: 21593341]
29. Reddy VB, et al. Redefining the concept of protease-activated receptors: cathepsin S evokes itch via activation of Mrgprs. Nat Commun. 2015; 6:7864. [PubMed: 26216096]
30. Stantcheva KK, et al. A subpopulation of itch-sensing neurons marked by Ret and somatostatin expression. EMBO Rep. 2016
31. Seal RP, et al. Injury-induced mechanical hypersensitivity requires C-low threshold mechanoreceptors. Nature. 2009; 462:651–655. [PubMed: 19915548]
32. Lou S, Duan B, Vong L, Lowell BB, Ma Q. Runx1 controls terminal morphology and mechanosensitivity of VGLUT3-expressing C-mechanoreceptors. J Neurosci. 2013; 33:870–882. [PubMed: 23325226]
33. Zylka MJ, Rice FL, Anderson DJ. Topographically distinct epidermal nociceptive circuits revealed by axonal tracers targeted to Mrgprd. Neuron. 2005; 45:17–25. [PubMed: 15629699]
34. Knop E, Korb DR, Blackie CA, Knop N. The lid margin is an underestimated structure for preservation of ocular surface health and development of dry eye disease. Developments in ophthalmology. 2010; 45:108–122. [PubMed: 20502031]
35. Cevikbas F, et al. A sensory neuron-expressed IL-31 receptor mediates T helper cell-dependent itch: Involvement of TRPV1 and TRPA1. J Allergy Clin Immunol. 2014; 133:448–460. [PubMed: 24373353]
36. Lee MG, et al. Agonists of the MAS-related gene (Mrgs) orphan receptors as novel mediators of mast cell-sensory nerve interactions. J Immunol. 2008; 180:2251–2255. [PubMed: 18250432]
37. Morita T, et al. HTR7 Mediates Serotonergic Acute and Chronic Itch. Neuron. 2015; 87:124–138. [PubMed: 26074006]
38. Kim YS, et al. Central Terminal Sensitization of TRPV1 by Descending Serotonergic Facilitation Modulates Chronic Pain. Neuron. 2014; 81:873–887. [PubMed: 24462040]
39. Otsuki JA, Grassick R, Seymour D, Kind LS. The use of 3H serotonin release from mast cells of the mouse as an assay for mediator liberation. Immunol Commun. 1976; 5:27–39. [PubMed: 59700]
40. Razin E, et al. IgE-mediated release of leukotriene C4, chondroitin sulfate E proteoglycan, beta-hexosaminidase, and histamine from cultured bone marrow-derived mouse mast cells. The Journal of experimental medicine. 1983; 157:189–201. [PubMed: 6184439]
41. Panneton WM, Hsu H, Gan Q. Distinct central representations for sensory fibers innervating either the conjunctiva or cornea of the rat. Exp Eye Res. 2010; 90:388–396. [PubMed: 20004193]
42. Zhao ZQ, et al. Cross-inhibition of NMBR and GRPR signaling maintains normal histaminergic itch transmission. J Neurosci. 2014; 34:12402–12414. [PubMed: 25209280]
43. Fleming MS, et al. The majority of dorsal spinal cord gastrin releasing peptide is synthesized locally whereas neuromedin B is highly expressed in pain- and itch-sensing somatosensory neurons. Molecular Pain. 2012; 8:52. [PubMed: 22776446]
44. Mishra SK, Holzman S, Hoon MA. A nociceptive signaling role for neuromedin B. The Journal of neuroscience : the official journal of the Society for Neuroscience. 2012; 32:8686–8695. [PubMed: 22723708]
45. Binshtok AM, Bean BP, Woolf CJ. Inhibition of nociceptors by TRPV1-mediated entry of impermeant sodium channel blockers. Nature. 2007; 449:607–610. [PubMed: 17914397]
46. Roberson DP, et al. Activity-dependent silencing reveals functionally distinct itch-generating sensory neurons. Nat Neurosci. 2013; 16:910–918. [PubMed: 23685721]
47. Wilson SR, et al. TRPA1 is required for histamine-independent, Mas-related G protein-coupled receptor-mediated itch. Nature neuroscience. 2011; 14:595–602. [PubMed: 21460831]
48. McNeil BD, et al. Identification of a mast-cell-specific receptor crucial for pseudo-allergic drug reactions. Nature. 2014
49. Mousli M, et al. Activation of rat peritoneal mast cells by substance P and mastoparan. J Pharmacol Exp Ther. 1989; 250:329–335. [PubMed: 2473189]

50. Parra A, et al. Ocular surface wetness is regulated by TRPM8-dependent cold thermoreceptors of the cornea. Nat Med. 2010; 16:1396–1399. [PubMed: 21076394]

51. Belmonte C, Aracil A, Acosta MC, Luna C, Gallar J. Nerves and sensations from the eye surface. Ocul Surf. 2004; 2:248–253. [PubMed: 17216099]

52. Abila B, Ezeamuzie IC, Igbigbi PS, Ambakederemo AW, Asomugha L. Effects of two antihistamines on chloroquine and histamine induced weal and flare in healthy African volunteers. Afr J Med Med Sci. 1994; 23:139–142. [PubMed: 7625301]

Methods-only References

53. McCoy ES, et al. Peptidergic CGRPalpha primary sensory neurons encode heat and itch and tonically suppress sensitivity to cold. Neuron. 2013; 78:138–151. [PubMed: 23523592]

54. Liu Q, et al. Molecular genetic visualization of a rare subset of unmyelinated sensory neurons that may detect gentle touch. Nat Neurosci. 2007; 10:946–948. [PubMed: 17618277]

55. Han L, et al. A subpopulation of nociceptors specifically linked to itch. Nat Neurosci. 2013; 16:174–182. [PubMed: 23263443]

56. Huang CC, et al. A histamine-independent itch pathway is required for allergic ocular itch. J Allergy Clin Immunol. 2016; 137:1267–1270. e1261–1266. [PubMed: 26521042]

57. Liu Q, et al. Sensory Neuron-Specific GPCR Mrgprs Are Itch Receptors Mediating Chloroquine-Induced Pruritus. Cell. 2009:1353–1365. [PubMed: 20004959]

58. Morita T, et al. HTR7 Mediates Serotonergic Acute and Chronic Itch. Neuron. 2015; 87:124–138. [PubMed: 26074006]

59. Dell, et al. Sample size determination. ILAR J. 2002; 43(4):207–13. [PubMed: 12391396]

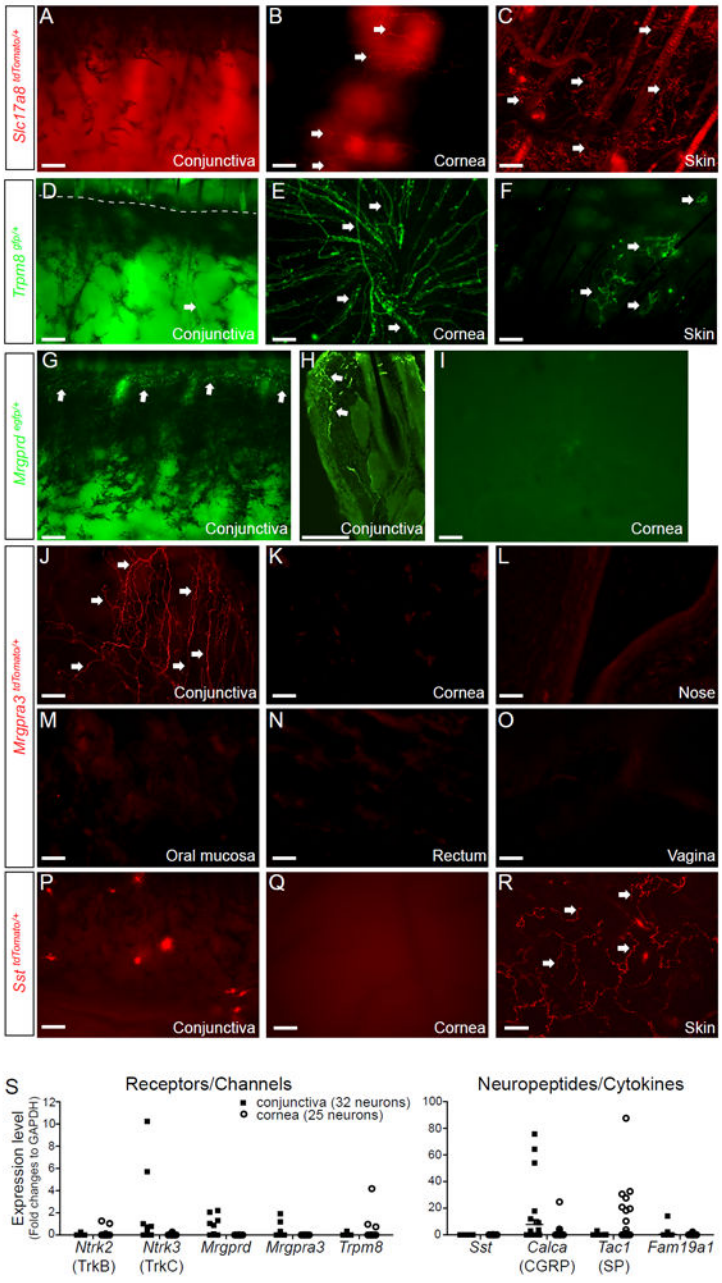

Fig. 1.

Distinct sensory innervation patterns between the cornea and conjunctiva. (**A-C**) Representative images showing the innervation patterns of type C low-threshold mechanoreceptors (C-LTMRs) that express vesicular glutamate transporter 3 (VGLUT3, gene *Slc17a8*) in the whole-mount cornea, conjunctiva, and skin from $Slc17a8^{Cre/+}$; $Rosa26^{tdTomato/+}$ ($Slc17a8^{tdTomato/+}$) mice. Arrows indicate *SLC17A8*-expressing fibers. (**D-F**) Representative images showing the innervation patterns of cold-sensitive C fibers that express TRPM8 in the whole-mount conjunctiva, cornea and skin from $Trpm8^{gfp/+}$ mice. Arrows indicate $TRPM8^{+}$fibers. The dashed line in **D** indicates the boundary between the

conjunctiva and eyelid skin. (**G-I**) Representative images showing the innervation patterns of MrgprD$^+$ sensory fibers in the conjunctiva (**G**, whole-mount; **H**, section) and whole-mount cornea (**I**)from *Mrgprd*$^{gfp/+}$ mice. Arrows indicate MrgprD$^+$fibers. (**J-O**) Representative images showing the innervation patterns of MrgprA3$^+$ sensory fibers in the whole-mount palpebral conjunctiva, cornea, nose, oral mucosa, rectum and vagina from *Mrgpra3*$^{cre/+}$;*Rosa26*$^{tdTomato/+}$ (*Mrgpra3*$^{tdTomato/+}$) mice. (**P-R**) Representative images showing the innervation patterns of somatostatin (SST)-expressing sensory fibers in the whole-mount conjunctiva, cornea and skin from *Sst*$^{Cre/+}$;*Rosa26*$^{tdTomato/+}$ (*Sst*$^{tdTomato/+}$) mice. Arrows indicate SST$^+$ fibers. All images shown are representatives of three independent experiments using tissues from at least 3 different mice. Scale bars: 100 μm. (**S**) Single cell qRT-PCR of trigeminal ganglion neurons retrogradely labeled from the cornea or conjunctiva. Each dot represents one sensory neuron. One data point of *Tac1* (995.48 in the cornea group) is outside the axis limits. data are expressed as mean±s.e.m.

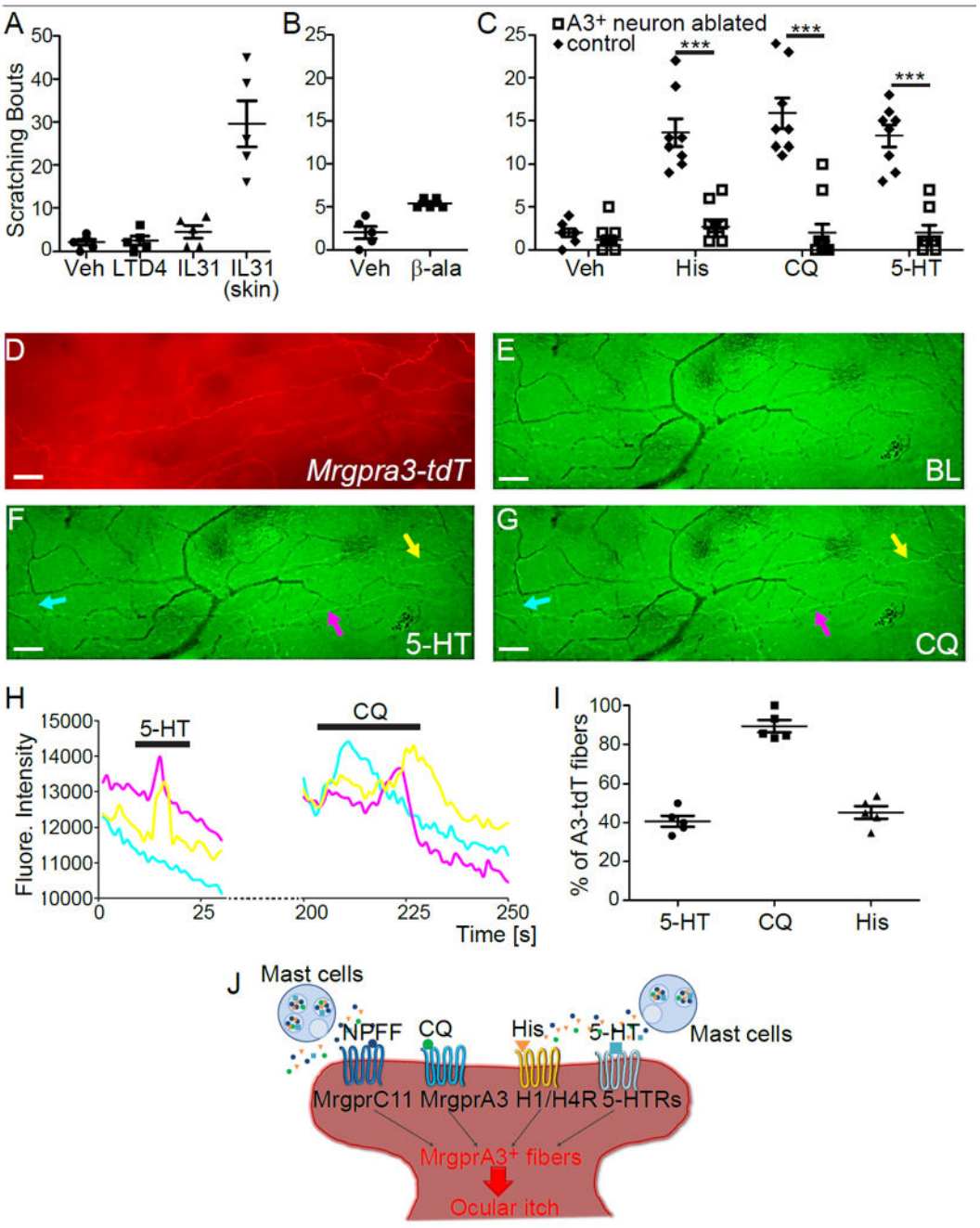

Fig. 2.

Conjunctival MrgprA3$^+$ sensory neurons mediate acute ocular itch. (**A**) Scratching response induced by conjunctival application of leukotriene D_4 (LTD_4, 10 pmole in 2.5 μl), interleukin 31 (IL-31, 25 pmole in 2.5 μl), or nape intradermal injection of IL-31 (100 pmole in 50 μl) in WT mice (n=5/group). (**B**) Ocular scratching responses evoked by saline vehicle and beta-alanine (500 nmole in 2.5 μl) in WT mice (n=5/group). (**C**) Ocular scratching responses induced by histamine (250 nmole in 2.5 μl), chloroquine (24 nmole in 2.5 μl), serotonin (940 pmole in 2.5 μl) in MrgprA3$^+$ neuron-ablated (n=11/group for histamine and chloroquine assays, and n=9 for serotonin assay)and WT mice (n=8/group). Statistical

analysis by two tailed Student's *t*-test (histamine, ***P=0.0001; chloroquine, ***P=0.000001; serotonin, ***P=0.000007). (**D**) Representative images showing MrgprA3^{+} fibers (labeled by tdTomato, red) in the conjunctiva from *Pirt*$^{GCaMP3/+}$; *Mrgpra3*^{tdTomato} mice (n=3). (**E-G**) Representative images showing the fluorescence changes of GCaMP3 in the conjunctival sensory fibers upon stimulation with serotonin (100 μM) and chloroquine (2 mM). Scale bars: 50 μm. (**H**) shows Ca^{2+} transients of representative MrgprA3^{+} sensory fibers (highlighted by colored arrows in **F-G**). (**I**) Percentages of MrgprA3-tdTomato sensory fibers that were activated by different pruritogens (5-HT: 40.7±2.5%, CQ: 89.4±2.8%, His: 45.3±2.9%). Each dot represents a conjunctiva explant from *Pirt*$^{GCaMP3/+}$; *Mrgpra3*^{tdTomato} mouse (n=5 conjunctivae from three mice per group). (**J**) Diagram showing the actions of both histamine and non-histamine pruritogens converge onto MrgprA3^{+} sensory fibers to induce ocular itch. All data are expressed as mean±s.e.m.

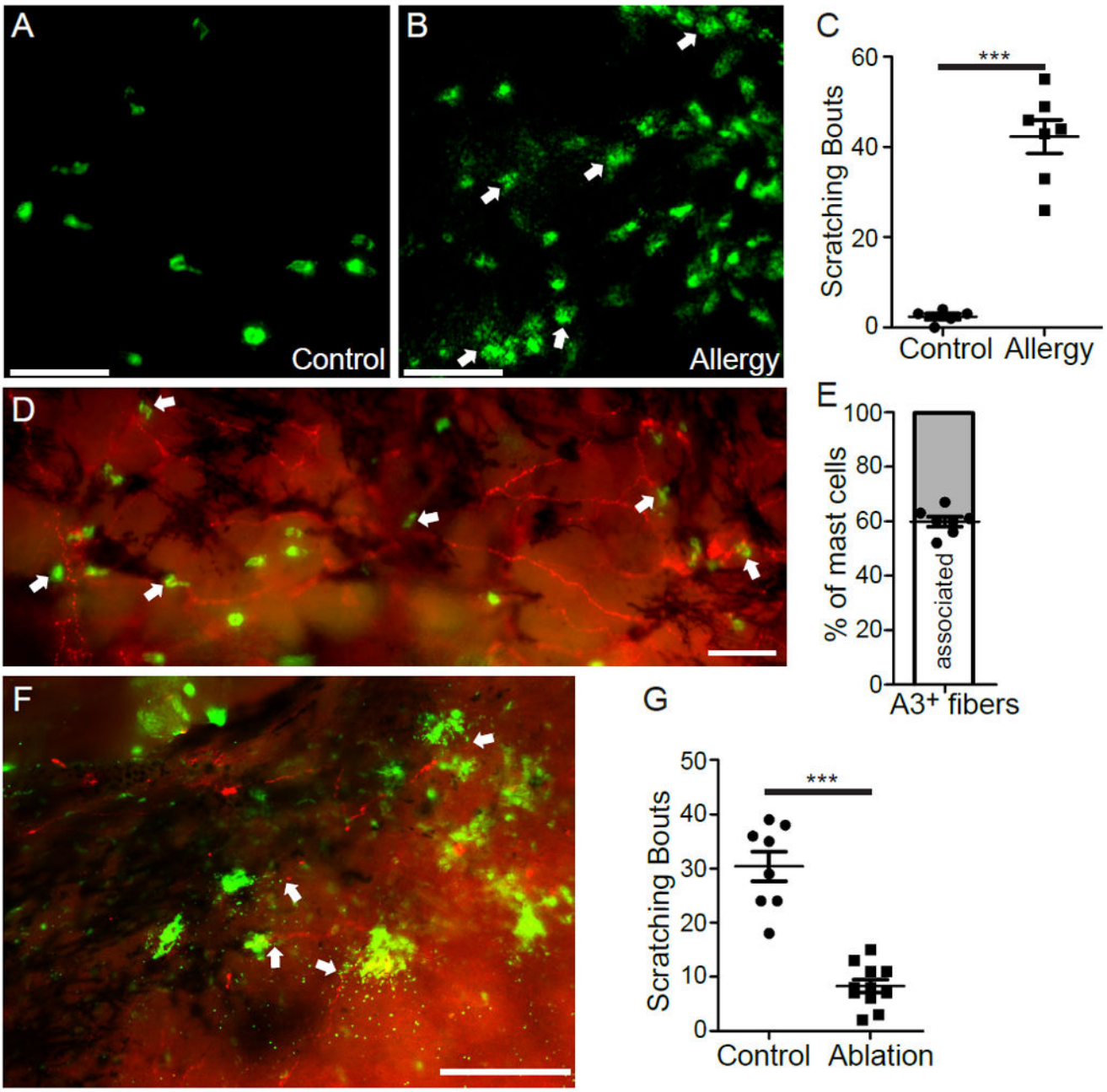

Fig. 3.

MrgprA3^{+} sensory neurons are required for mast cell-dependent allergic ocular itch. (**A-B**) Representative images of mast cells (stained with FITC-avidin, green) in the whole-mount conjunctivae of non-immunized (**A**) and immunized mice (**B**). Arrows indicate the granules released from mast cell bodies upon challenging with allergen ovalbumin. (**C**) Ocular scratching responses evoked by topical conjunctival application of allergen ovalbumin in non-allergic control mice (n=5) and allergic mice (n=7). Statistical analysis by two tailed Student's *t*-test (***P=0.00003). (**D**) Representative image of the whole-mount conjunctiva

from *Mrgpra3*^{tdTomato} mice. Arrows indicated avidin-stained mast cells. (**E**) The proportion of mast cells closely associated with MrgprA3^{+} sensory fibers (n=7 conjunctival explants) (**F**) Representative image showing the interaction between released granules (green) and MrgprA3^{+} sensory fibers (red) in the conjunctiva upon allergen challenge, as indicated by arrows. All images shown are representatives of three independent experiments using tissues from at least 3 different mice. Scale bars: 50 μm. (**G**) Ocular scratching responses induced by mast cell-dependent ocular allergy in MrgprA3^{+} neuron-ablated mice (n=11) and control *Rosa26*$^{HBEGF/+}$ mice (n=8). Statistical analysis by two tailed Student's *t*-test (***P=0.0000003). All data are expressed as mean±s.e.m.

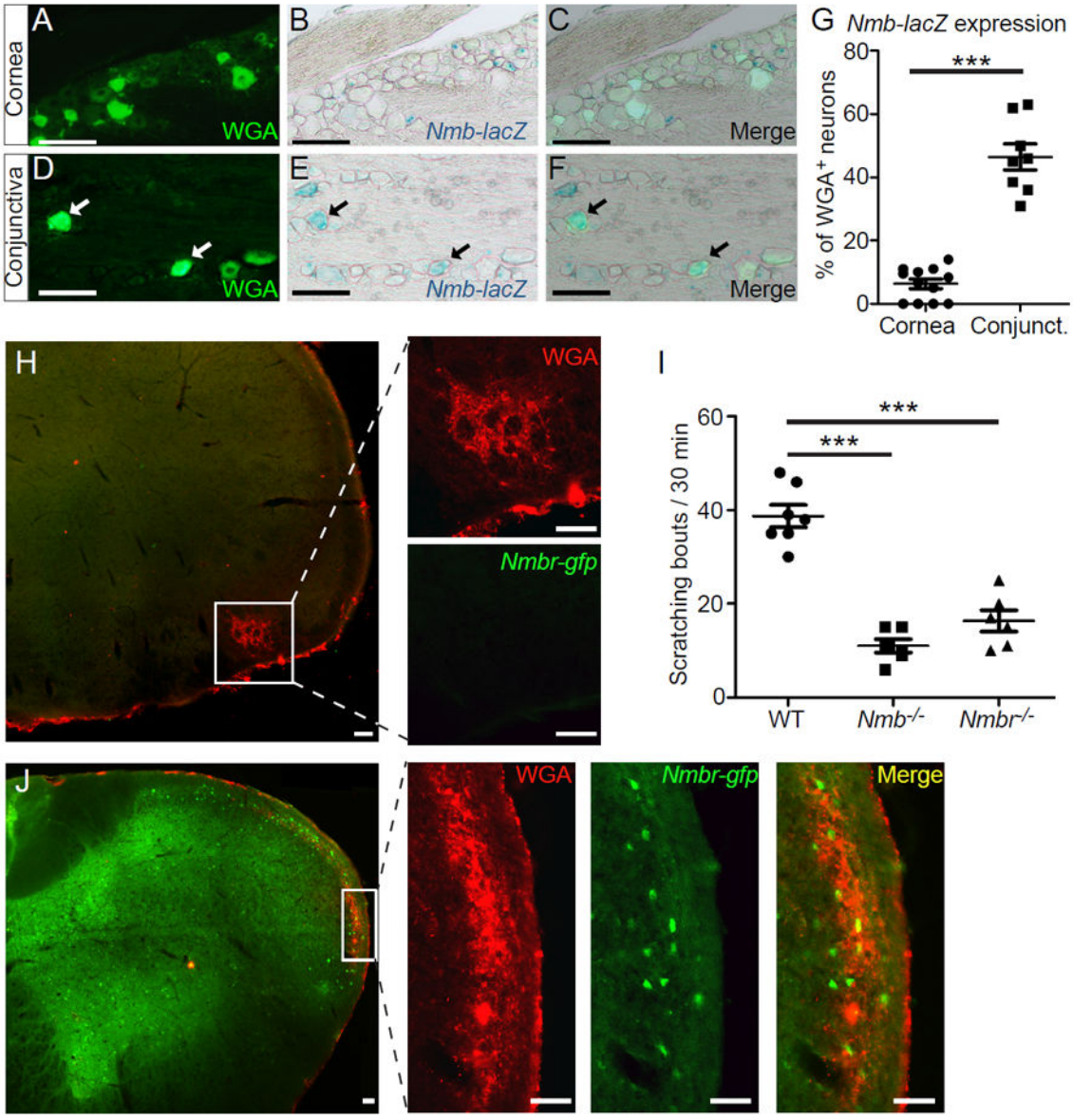

Fig. 4.

Central NMB/NMBR signaling is required for conjunctival itch transmission. (**A-G**) Representative images showing x-gal staining of *Nmb*-lacZ reporter in sections containing sensory neurons retrogradely labeled by Wheat Germ Agglutinin conjugated with Alexa Fluor™ 488 (WGA-488) from the conjunctiva or cornea of *Nmb*$^{tm1.1(KOMP)Vlcg}$ mice. Each dot in (**G**) represents one section image of trigeminal ganglia (n=6 TGs from three mice per group). Statistical analysis by two tailed Student's *t*-test (***P=0.000008). (**H, J**) Representative images showing the absence or presence of *Nmbr*-GFP in the central projection area of corneal (**H**) or conjunctival afferent neurons (**J**). Scale bars: 50 μm. (**I**) Ocular scratching responses evoked by ocular allergy in *Nmb*$^{-/-}$ mice (n=5), *Nmbr*$^{-/-}$ mice (n=6) and WT (control) mice (n=7). Statistical analysis by one-way ANOVA followed by

two tailed Student's *t*-test (*Nmb*$^{-/-}$ vs. WT, ***P=0.000002; *Nmbr*$^{-/-}$ vs. WT, ***P=0.00004). All data are expressed as mean±s.e.m.

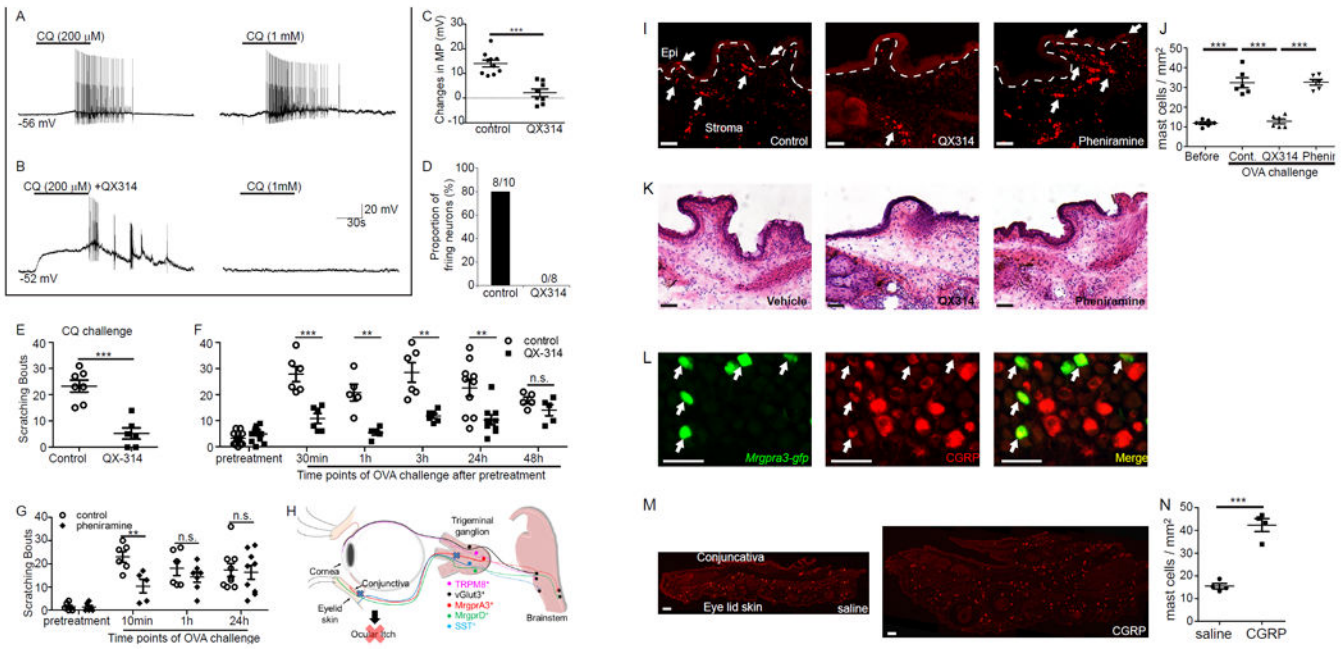

Fig. 5.

Pharmacological silencing of MrgprA3$^+$ neurons reduces both acute and allergic ocular itch. (**A**) Representative traces of action potentials elicited by repeated chloroquine (CQ) application were chosen from 10 recorded MrgprA3$^+$ sensory neurons in the control group. (**B**) Representative traces of action potentials induced by application of QX-314 plus CQ and subsequent CQ alone were chosen from 8 recorded MrgprA3$^+$ neurons in the QX-314 group. (**C**) Changes in the membrane potential (MP) in control (n=10) and QX-314 (n=8) groups.Statistical analysis by two tailed Student's *t*-test (***P=0.00003). (**D**) The proportion of firing neurons in control and QX-314 groups. (**E**) Ocular scratching responses induced by conjunctival application of CQ (12 mM) after pretreatments of 4mM CQ and 1% QX-314 (QX-314 group, n=6), compared with the control group pretreated with 4 mM CQ alone (n=7). Statistical analysis by two tailed Student's *t*-test (***P=0.0001). (**F**) Allergen ovalbumin (OVA)-induced ocular scratching responses at different time points after pretreatment of 4mM CQ and 1% QX-314, compared with controls pretreated with 4 mM CQ alone (n=14 (pre-treatment), 6 (30min), 5 (1h), 6 (3h), 10 and 9 (24h), 5 (48h) mice/group). Statistical analysis by two tailed Student's *t*-test (30min, ***P=0.0006; 1h, **P=0.007; 3h, **P=0.006; 24h, **P=0.006). (**G**) Allergen ovalbumin (OVA)-induced ocular scratching responses at different time points after pretreatment of pheniramine (0.4%, 2 μl) or vehicle control (n=6 (pre-treatment), 6 and 5 (10min), 6 and 7 (1h), 9 (24h) mice/group). Statistical analysis by two tailed Student's *t*-test (**P=0.007). (**H**) A diagram summarizing the predominant role of MrgprA3$^+$ sensory neurons in ocular itch. (**I**) Representative images of vehicle-treated (control), QX-314-treated and pheniramine-treated conjunctivae under allergic conjunctivitis. The dashed lines indicate the boundary between the epithelium and stroma of the conjunctivae; white arrows indicate the mast cells. (**J**) Quantitative analysis of mast cell number after different treatments (each dot represents a conjunctiva explant; n=6 conjunctivae from three mice per group).Statistical analysis by

one-way ANOVA followed by two tailed Student's *t*-test (before vs. cont. ***P=0.0003; cont. vs. QX314 ***P=0.00004; QX314 vs. phenir ***P=0.000001) (**K**) Representative H&E staining showing inflammatory cell infiltration in vehicle, QX-314 and pheniramine-treated allergic conjunctiva after allergen (OVA) challenges. (**L**) Representative images showing the expression of neuropeptide CGRP (red) in MrgprA3^{+} sensory neurons (green), as indicated by arrows. (**M**) Representative images showing mast cell in the conjunctivae after treatments of CGRP (0.5 nmol in 2.5 μl) or saline. (**N**) Quantitative analysis of mast cell number after CGRP treatments (each dot represents a conjunctiva explant; n=4 conjunctivae from three mice per group). Statistical analysis by two tailed Student's *t*-test (***P=0.0001). All data are expressed as mean±s.e.m. All images shown are representatives of three biologically independent mice.Scale bars: 50 μm

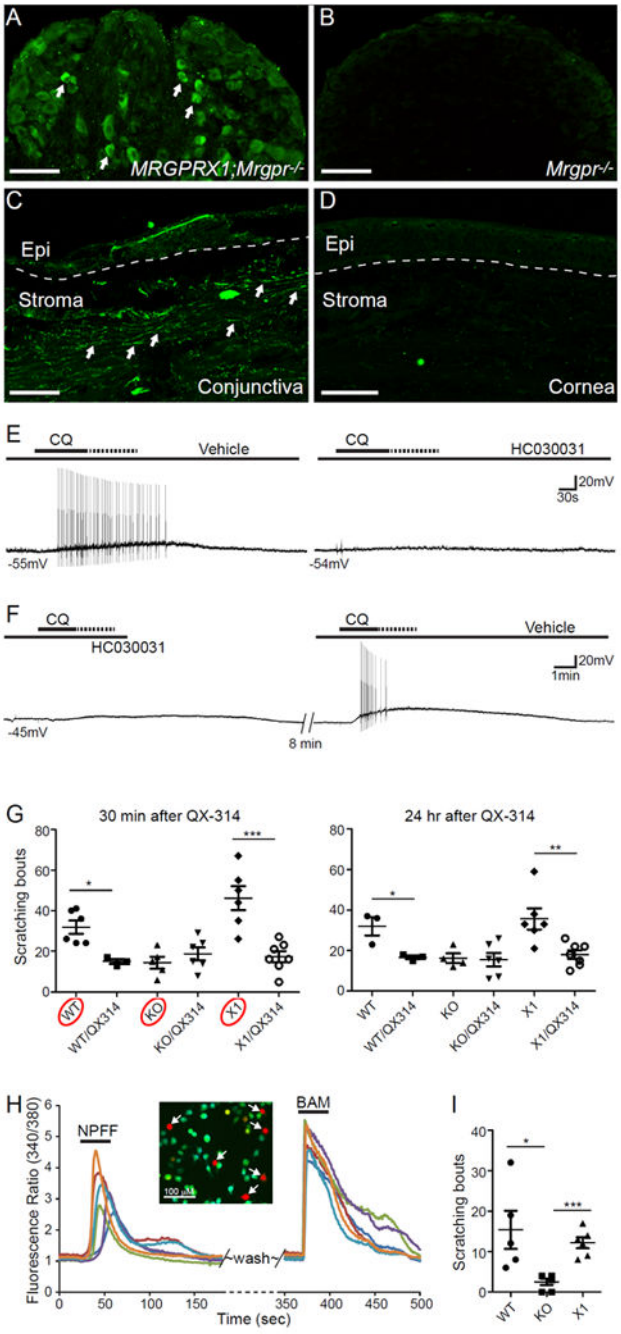

Fig.6.

MrgprX1^{+} sensory afferents selectively innervate human conjunctiva and mediate itch in a humanized mouse model. (**A-B**) Representative images showing immunofluorescent staining of sensory neurons from *MRGPRX1;Mrgpr-clusterΔ*$^{-/-}$and *Mrgpr-clusterΔ*$^{-/-}$ mice using a newly generated antibody for hMrgprX1. Arrows indicate sensory neurons labeled by hMrgprX1 antibody. (**C-D**) Representative images showing immunofluorescent staining of human conjunctiva and cornea using hMrgprX1 antibody. Arrows indicate sensory fibers labeled by hMrgprX1 antibody. The dashed lines indicate the boundary between the

epithelium and stroma. Images shown are representative of three biologically independent samples. Scale bars: 100 μm. (**E-F**) Representative traces of action potentials elicited by CQ (1 mM) stimulation in hMrgprX1-expressing sensory neurons (as determined by calcium imaging using BAM8-22, n=5). The recorded neurons received pretreatments of vehicle control and 100 μM HC030031 (100 μM) (**E**) or in reverse order (**F**). (**G**) Scratching responses induced by conjunctiva challenge of allergen OVA in immunized WT, *Mrgpr-clusterΔ*$^{-/-}$, and *MRGPRX1;Mrgpr-clusterΔ*$^{-/-}$ mice with or without pretreatments of 1% QX-314 with 4mM chloroquine (30min, n=6 and 3 (WT group), 5 and 6 (KO group), 6 and 7 (X1 group); 24hr, n=3 and 3 (WT group), 4 and 6 (KO group), 6 and 7 (X1 group)). Statistical analysis by two tailed Student's *t*-test (WT vs. WT/QX314, 30min *P=0.011, 24hr *P=0.03; X1 vs. X1/QX314, 30 min ***P=0.0007; 24hr, **P=0.007). (**H**) Representative calcium transients of hMrgprX1-expressing heterologous cells in response to NPFF (6 μM) and BAM8-22 (2 μM). Arrows indicate BAM8-22 responsive hMrgprX1-expressing cells that were activated by NPFF. (**I**) Scratching responses induced by conjunctival application of NPFF (2.5 nmole in 2.5 μl) in WT (n=5), *Mrgpr-clusterΔ*$^{-/-}$ (n=6), and *MRGPRX1;Mrgpr-clusterΔ*$^{-/-}$ mice (n=6). Statistical analysis by one-way ANOVA (p=0.0082) followed by two tailed Student's *t*-test (WT vs. KO, *p=0.016; KO vs. X1, ***p=0.0001). All data are expressed as mean±s.e.m.